Research Article

Sulfachloropyridazine as an Eco-Friendly Inhibitor for Corrosion of Mild Steel in H_2SO_4 Solution

Omar A. Hazazi[1], Ahmed Fawzy[1,2] and Mohamed I. Awad[1,3,*]

[1] Chemistry Department, Faculty of Applied Sciences, Umm Al-Qura University, Makkah Al-Mukarramah, Saudi Arabia Kingdom
[2] Chemistry Department, Faculty of Science, Assiut University, Assiut, Egypt
[3] Chemistry Department, Faculty of Science, Cairo University, Gizah, Egypt

Abstract

The anticorrosion characteristics of sulfachloropyridazine (SCP) as an eco-friendly inhibitor for the corrosion of mild steel in 0.5 M H_2SO_4 solution has been studied, for the first time, using potentiodynamic measurements and electrochemical impedance spectroscopy (EIS). The possible synergistic effect of halide ions on the inhibitive effect of SCP has been investigated. Thermodynamic calculations indicated that SCP adsorption on steel surface obeyed Langmuir adsorption isotherm. Electrochemical measurements showed that the SCP acted mainly as an anodic inhibitor. Halides significantly promoted the inhibition performance of SCP through the pre-adsorption on the electrode surface which is positively charged under the present conditions.

Keywords: Corrosion, Green inhibitor, mild steel, synergism, Eco-friendly

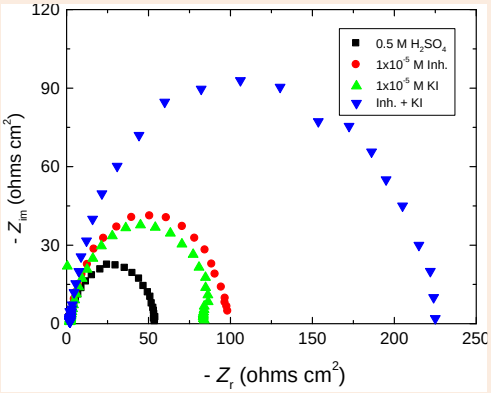

***Correspondence**
Author: Mohamed I Awad
Email: mawad70@yahoo.com

Introduction

Carbon steel is the primary material used in many applications such as cooling water systems and other industrial water distribution systems. Carbon steel suffers from the relatively limited corrosion resistance. On the other hand acids are used for descaling and removing of corrosion products. In acid media steel should be protected from the further attack of the harsh environment. In this correspondence organic inhibitors are usually added to inhibit the corrosion of steel during pickling. Organic inhibitors contain hetero atoms such as oxygen, nitrogen, sulfur and phosphorous. In addition, they also contain double bonds, triple bonds and aromatic rings. All these enhance the adsorption process and result in the formation of an effective coating on the surface of the metal. This coating forms a barrier between metal and the corrosive environment and protects the metal from undergoing corrosion [1-12].

For the reason of increasing environmental protection, green inhibitors became very popular, ‘‘green’’ corrosion inhibitors has been addressed toward the goal of using cheap, effective molecules at low or ‘‘zero’’ environmental impact [13]. Over the years, many scientists tried to find suitable green corrosion inhibitors in various corrosive media [14-17]. These compounds include for examples certain amino acids and derivatives [18, 19], ascorbic acid [20], succinic acid [21], tryptamine [22], caffeine [23] and extracts of natural substances [24-27]. In the present work the inhibitive action of an eco-friendly compound on the corrosion of mild steel in 0.5 M H_2SO_4 is studied. The possible synergistic action of halides on the inhibitive action of SCP is also investigated. Potentiodynamic measurements and impedance spectroscopy are used for this purpose. Subsequently, thermodynamic factors are derived.

Experimental

Materials and Methods

Mild Steel Sample: Tests were performed on mild steel of the following composition (wt. %): 0.07% C, 0.29% Mn, 0.07% Si, 0.012% S, 0.021% P and the remainder iron. Samples of 0.5 cm^2 were used.
Inhibitor: Sulfachloropyridazine (SCP) of structure shown in **Figure** 1, sodium halides were obtained from Sigma-Aldrich and used as received.

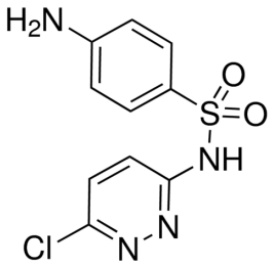

Figure 1 Structure of sulfachloropyridazine (SCP)

Solutions: The solution of 0.5 M H_2SO_4 was prepared by dilution of AR grade 98% H_2SO_4. Stock solutions of SCP and sodium halides were prepared in 0.5 M H_2SO_4 and the desired concentrations were obtained by appropriate dilution.

Electrochemical Measurements: Electrochemical experiments were carried out in a conventional three-electrode cell with a platinum counter electrode (CE) and $Hg/Hg_2SO_4/SO_4^{2-}$ coupled to a fine Luggin capillary as a reference electrode (RE). In order to minimize the ohmic contribution, the Luggin capillary was kept close enough to the working electrode (WE) which was fitted into a glass tube of proper internal diameter by using epoxy resins. The WE surface area of 0.5 cm^2 was abraded with emery paper down to 2000 on test face, rinsed with distilled water, degreased with acetone, and dried with a cold air stream. Before measurements the electrode was immersed in the test solution at open circuit potential (OCP) for 15 min at 25 ^oC or until the steady state is obtained. All electrochemical measurements were carried out using PGSTAT30 potentiostat/galvanostat. The potential of potentiodynamic polarization curves was done from a potential of -250 mV vs. OCP, to 250 mV vs. OCP at a scan rate of 2 mV/s. Current densities were calculated on the basis of the apparent geometrical surface area of the electrode. The measurements were repeated at least three times to test the reproducibility of the results. The open circuit potentials (OCP) of samples in 0.5 M H_2SO_4 solution were measured against the reference electrode for 60 min.

Results and Discussion

The variation of open circuit potential of mild steel as a function of exposure time (E_{OCP} - t) in 0.5 M H_2SO_4 in the absence and presence of 10 μM SCP is presented in **Figure** 2. Several interesting points can be extracted from this **figure**;

1. The E_{OCP} in the blank solution shifted anodically towards the steady state which is obtained after *ca*. 10 min. This positive shift is attributed to the initial dissolution process of the air formed oxide film and the attack on the bare metal.
2. In the presence of the inhibitor, the E_{OCP} shifted initially to positive potentials compared with that in the absence of inhibitor and then shifted cathodically. The initial positive shift could be attributed to the adsorption of the inhibitor and the partial attraction of electrons by the electronegative nitrogen in the inhibitor decreasing the electron density on the iron.

3. The steady state is attained faster in the presence of the inhibitor compared with the blank response. With increasing the concentration of the inhibitor the anodic shift in the open circuit potential increases (see Table 1, Column 1) indicating that the inhibitor might act mainly as an anodic inhibitor. It has been reported that E_{OCP} displacement could be utilized as a diagnosis of the type of the inhibitor; if E_{OCP} is at least ±85 mV different to the one measured in the blank solution it can be classified as an anodic or cathodic inhibitor [28, 29]. In the present case, the maximum shift is around 56 mV (obtained in the presence of 200 μM of SCP) revealing that the present inhibitor acts as a mixed type inhibitor with a preferential restrain on the anodic process.

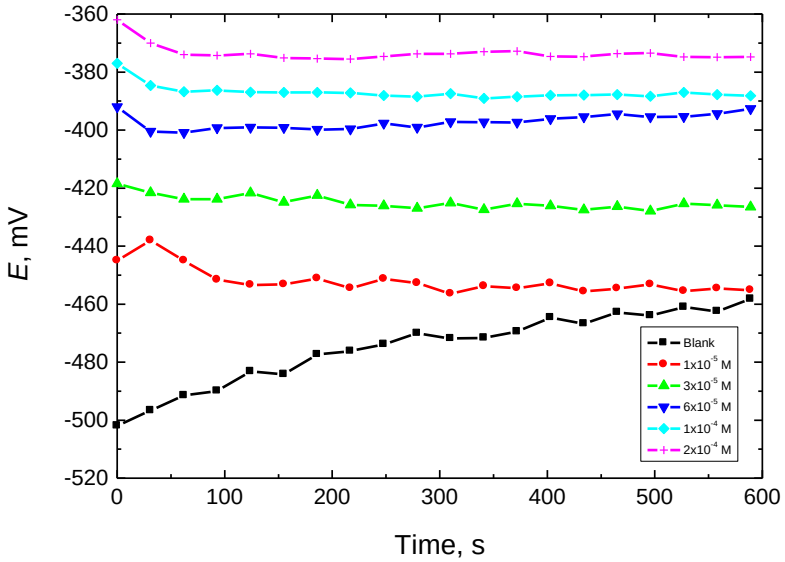

Figure 2 Open circuit potential, E_{OCP} vs. time, for mild steel immersed in 0.5 M H_2SO_4 (Blank) in the absence and presence of 10 μM SCP at 25 °C.

Figure 3 shows the polarization curves of mild steel obtained in 0.5 M H_2SO_4 in the absence and presence of various concentrations of SCP at 25 °C. The various associated electrochemical parameters extracted from this **figure** such as the corrosion potential, E_{corr}, corrosion current density, i_{corr}, Tafel slopes, b_c and b_a and the percentage inhibition are given in **Table** 1. As can be seen the effect of SCP on the cathodic branch is negligible, while the effect on the anodic branch is tremendous; the anodic branch bodily shifted to lower currents. Also the corrosion potential shift to anodic direction and the shift increases with increasing SCP concentration consistently with the results shown in **Figure** 2. However, the effect of the inhibitor concentration on the Tafel slopes is negligible indicating that the inhibitor exerts its action via simple blocking, and that the adsorption of the inhibitor does not change the mechanism [30].
The protection efficiency is given by:

$$\%\, P = \left[1 - \frac{i_{corr1}}{i_{corr2}}\right] 100 \qquad (1)$$

where i_{corr1} and i_{corr2} are corrosion current densities in the absence and presence of inhibitor, respectively. **Figure** 4 shows the dependence of the protection efficiency on the concentration; the dependence is of sigmoid shape; i.e. %P increases with the concentration until it reaches a plateau at protection efficiency *ca*. 87 % indicating the significant inhibition efficiency of the present inhibitor under the present conditions.

For further insight into the corrosion inhibition process the corrosion behavior of mild steel in 0.5 M H_2SO_4 both in the presence and absence of SCP compound is investigated by the electrochemical impedance spectroscopy (EIS)

at 298 K after 30 min of immersion and shown in **Figure** 5. The charge-transfer resistance (R_t) values are calculated from the difference in the impedance at lower and higher frequencies [31]. Then the double layer capacitance (C_{dl}) is calculated using Eq. 2;

$$C_{dl} = \left[\frac{1}{2\pi f_{\max} R_{ct})} \right] x100 \qquad (2)$$

where f_{max} is the frequency at which the imaginary component of the impedance is maximal (Z_{max}). The inhibition efficiency is calculated from the following equation;

Table 1 Polarization data for mild steel in 0.5 M H_2SO_4 with sulfachloropyridazine

10^5 [SCP], M	E_{corr} (mV)	β_c (mV/dec)	B_a (mV/dec)	I_{corr} (μA/cm^2)	θ	% P
0	-458	92	83	199	--	--
1	-440	93	81	105	0.47	47
3	-425	95	79	68	0.65	65
6	-418	96	76	50	0.75	75
10	-412	99	75	34	0.82	82
20	-406	97	76	23	0.88	88

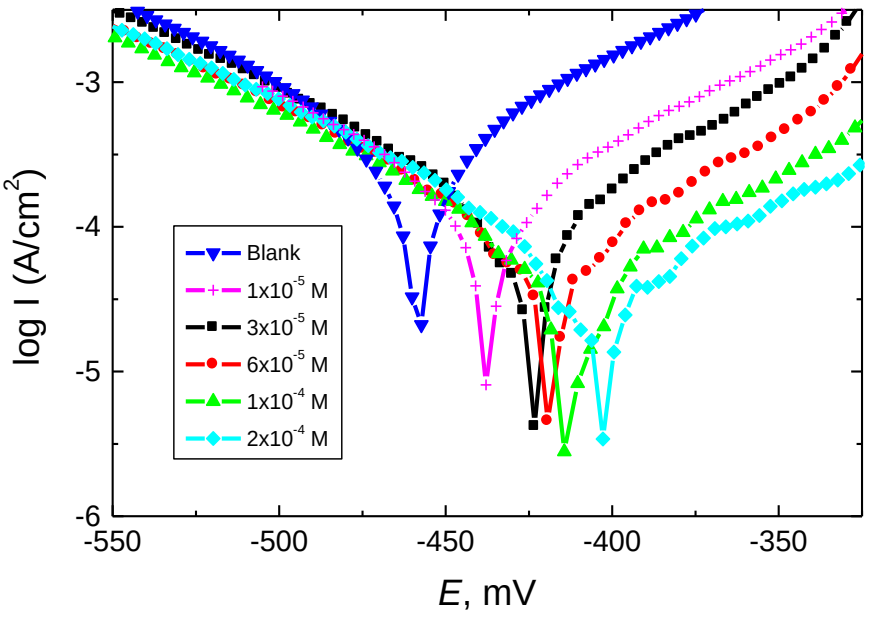

Figure 3 Potentiodynamic polarization curves for mild steel in 0.5 M H_2SO_4 in the absence and presence of different concentrations of SCP at 25 ºC.

$$\%P = \left[\frac{(1/R_t) - (1/R_{t/inh})}{(1/R_c)} \right] x100 \quad (3)$$

where R_t and $R_{t/inh}$ are the charge transfer-resistance values in the absence and presence of inhibitor, respectively. As can be seen from this figure, all the Nyquist plots contain slightly depressed semicircles with the center under the real axis. This implies that corrosion of the mild steel in 0.5 M H_2SO_4 solution mainly controlled by a charge-transfer process [32]. The deviation from pure semi-circle behavior known as frequency depression happens due to roughness and inhomogeneity of the surface during corrosion [33]. The increase of concentration of SCP increases the semicircle radius, obviously. Moreover, since the polarization resistance is attributed to the diameter of semicircles, and from the figure it is clear that the diameters of semicircles significantly increase with the increase in concentration. This is attributed to the increase in the substrate impedance with the increase in inhibitor concentrations.

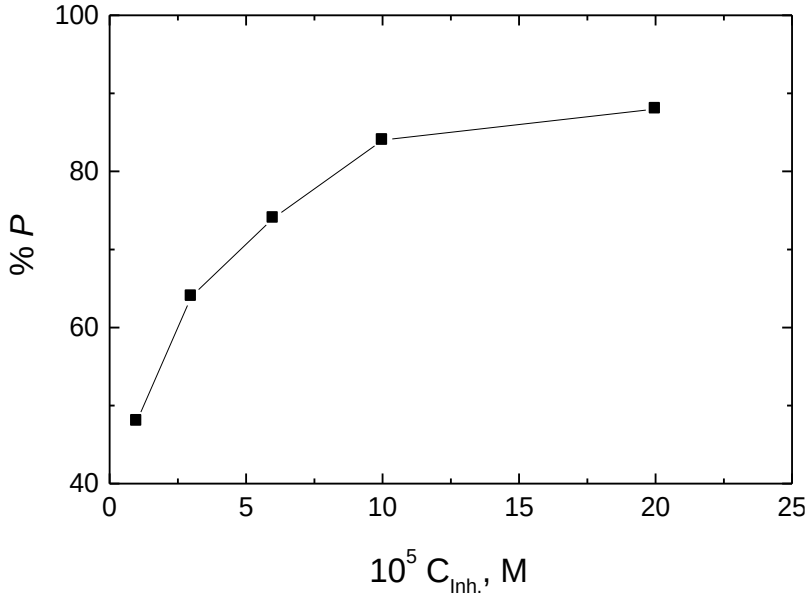

Figure 4 Dependence of protection efficiency of SCP on concentration.

Effect of Immersion Time

Figure 6 shows Nyquist impedance plots for the steel that was immersed in 0.5 M H_2SO_4 solutions containing 10 μM SCP at different time intervals; data in the absence of SCP is not shown. Increasing the immersion time of steel in the absence of SCP decreases the diameter and the value of |Z|, which indicates the corrosiveness action of the sulfuric acid that does not allow the steel surface to develop oxide layers or corrosion products and that effect increases with increasing time of contact between the acid and the steel. Interestingly the presence of SCP significantly increases both the diameter of the obtained semicircle and values of |Z| with increasing immersion time indicating the significant corrosion inhibition in the presence of SCP [34].

Synergism

Under the present conditions SCP inhibitor is expected to be protonated, i.e., positively charged (pK_{a1} and pK_{a2} equal 1.90 and 5.40, respectively [35]). Based on the potential of zero charge iron is expected to be positively charged [36]. Thus the adsorption of the positively charged inhibitor on the steel surface would be retarded. There are several controlling factor for the inhibiting effect of organic inhibitors such as the molecular structure of the organic

compounds, surface charge density and the potential of zero charge of the metal. The adsorption of positively charged inhibitor is expected to be enhanced by increasing the negative charge density on the metal surface. Thus the pre-adsorption of a halide could enhance the adsorption of the SCP inhibitor due to ion–pair interactions between the molecules and the halide ions, resulting in what is the so-called inhibition synergism. This interaction can be quantized by a parameter called synergism parameter (S_θ) [37] which is defined as,

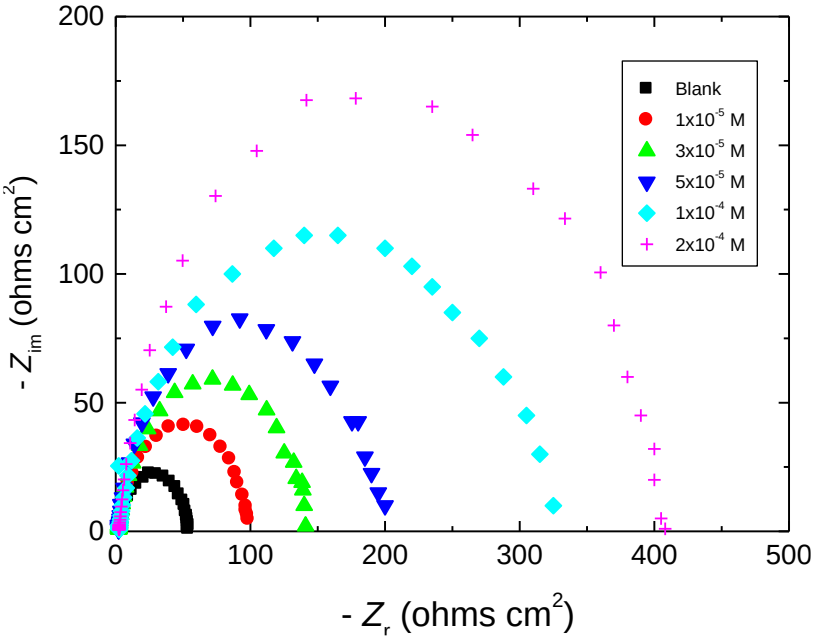

Figure 5 Nyquist plots of SCP on mild steel in 0.5 M H_2SO_4 25 ^oC.

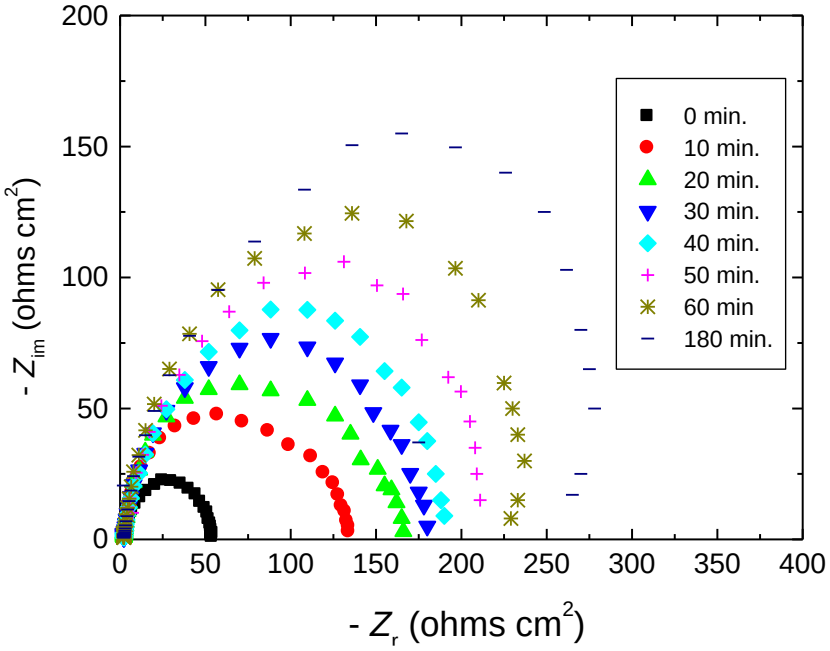

Figure 6 Nyquist plots of 1x10^{-5} M SCP on mild steel in 0.5 M H_2SO_4 at different time intervals.

$$S_\theta = \left[\frac{1-\theta_{1+2}}{1-\theta'_{1+2}}\right] x100 \qquad (4)$$

where $\theta_{1+2} = (\theta_1 + \theta_2) - (\theta_1\theta_2)$; θ_1 and θ_2 are the degrees of surface coverage in the individual presence of the halide ion and the SCP, respectively, and θ'_{1+2} is the degree of surface coverage in their coexistence. S_θ approaches unity when no interaction takes place between the inhibitor molecules and the halide ion, $S_\theta > 1$ and $S_\theta < 1$ denotes synergistic and antagonistic effects, respectively [38]. **Figure** 7 shows the impedance plots of mild steel in 0.5 M H_2SO_4 in the absence of halides and SCP, in the individual presence and in their coexistence, 10 μM each. Panels a, b and c are for chloride, bromide and iodide, respectively. The different electrochemical parameters are given in Table 2. As can be seen the inhibition efficiency in the presence of either halide or inhibitor is low as revealed from the small semicircles. However when both species are present, the radius of the impedance plots significantly increases, i.e., a significant increase in the inhibition efficiency, in the presence of very low concentration of both species, is obtained (as shown in Table 2). The extent of the enhancement is represented as synergistic parameters. In the presence of any of the studied halides the S_θ values are found to be higher than unity, suggesting a real synergistic action of halide ion with the inhibitor. The above results reveal that SCP can act effectively as a corrosion inhibitor in the presence of halide ions even at low concentrations of SCP (in the micromolar range). The obtained S_θ is in the order: $Cl^- < Br^- < I^-$ in agreement with literature [28, 39].

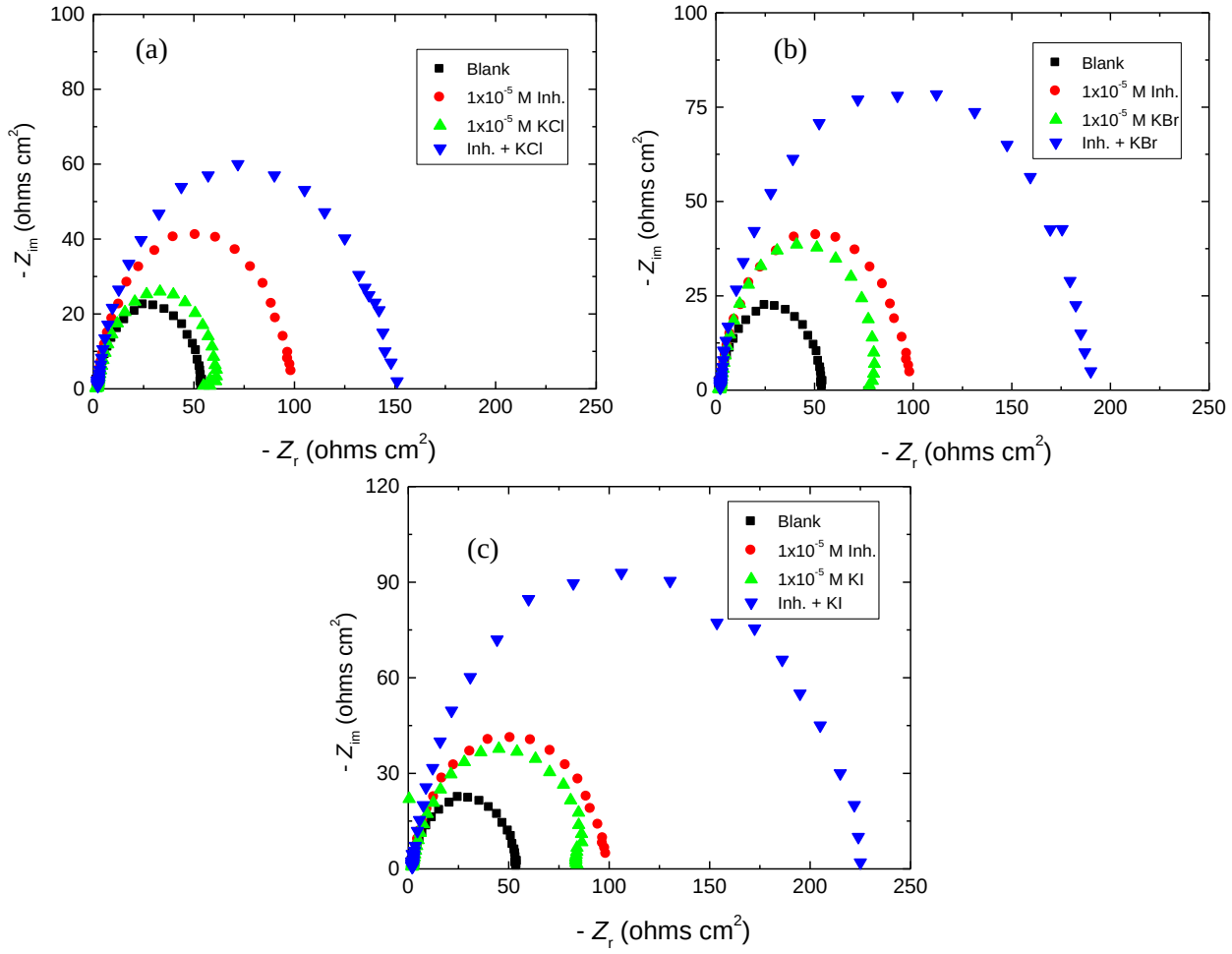

Figure 7(a-c) Nyquist plots of 1x10^{-5} M SCP on mild steel in 0.5 M H_2SO_4 in the absence and presence of 1x10^{-5} M of halide; panel (a) for KCl, panel (b) for KBr and panel (c) for KI.

Table 2 Polarization data and synergism parameter (S_θ) for SCP and halide ions on mild steel in 0.5 M H_2SO_4 at 25 °C.

System, $1x10^{-5}$ M	E_{corr} (mV)	β_c (mV/dec)	B_a (mV/dec)	I_{corr} (μA/cm^2)	% *P*	θ	S_θ
Blank	-458	92	83	199	--	--	
SCP	-440	93	81	105	47	0.47	
Cl^-	-451	95	71	171	15	0.15	**1.32**
SCP + Cl^-	-442	97	79	67	66	0.66	
Br^-	-455	91	79	143	31	0.31	**1.35**
SCP + Br^-	-441	95	77	53	73	0.73	
I^-	-451	96	73	123	39	0.39	**1.39**
SCP + I^-	-438	91	69	45	77	0.77	

Adsorption Isotherm

The adsorption of an inhibitor involves the substitution of the adsorbed water molecules ($H_2O_{(ads)}$) by the inhibitor molecules according to the following equation;

$$Org_{(sol)} + nH_2O_{(ads)} \rightarrow Org_{(ads)} + nH_2O_{(sol)} \quad (5)$$

where $Org_{(sol)}$ and $Org_{(ads)}$ are the organic molecules in the aqueous solution and the adsorbed one, respectively. *n* is the number of water molecules replaced by one inhibitor molecule. The basic information on the interaction between the inhibitor and the mild steel surface could be extracted from the so-called adsorption isotherms. Adsorption isotherms provide useful insights into the mechanism of corrosion inhibition. Fitting of the experimental data to various isotherms including Langmuir, Temkin, and Flory–Huggins isotherms has been examined, and it has been found that the experimental results in this study for SCP and SCP/halide ions systems accord with Langmuir isotherm, given by Eq. 6 [40], and the plots are presented in **Figures** 8 and 9 for SCP alone and SCP/halide, respectively.

$$\frac{C}{\theta} = \frac{1}{K} + C \quad (6)$$

where *K* is the equilibrium constant for adsorption process which reflects the extent of interaction between the inhibitor and the metal surface and *C* is the concentration of the inhibitor. The correlation coefficients and slopes confirm this assumption. Consequently Inhibitor exerts its action via the formation of monolayer, and there is no interaction between the inhibitor molecules [41]. The parameters derived from Langmuir, i.e. *K* and change in free energy of adsorption ΔG^o_{ads} are given in Table 3. The large value of *K* reflects the stronger ability of adsorption of the inhibitor on the metal surface. ΔG^o_{ads} was calculated using Eq. 7 [42];

$$\Delta G^o_{ads} = -RT \ln(55.5 K_{ads}) \quad (7)$$

where *R* is molar gas constant (8.314 J K^{-1}), *T* is temperature in Kelvin and value 55.5 is the concentration of water in mol dm^3 in solution.

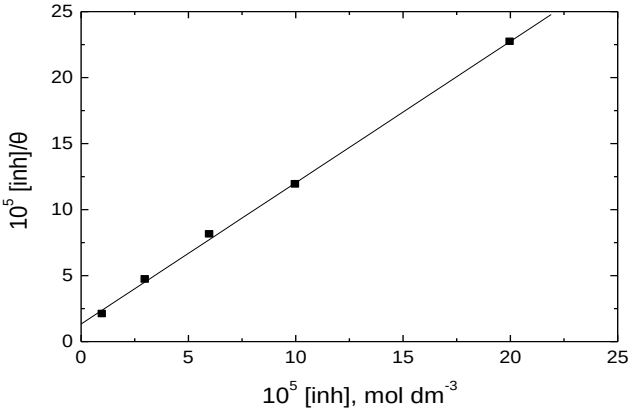

Figure 8 Langmuir adsorption isotherms for SCP on mild steel in 0.5 M H_2SO_4 at 25 ºC.

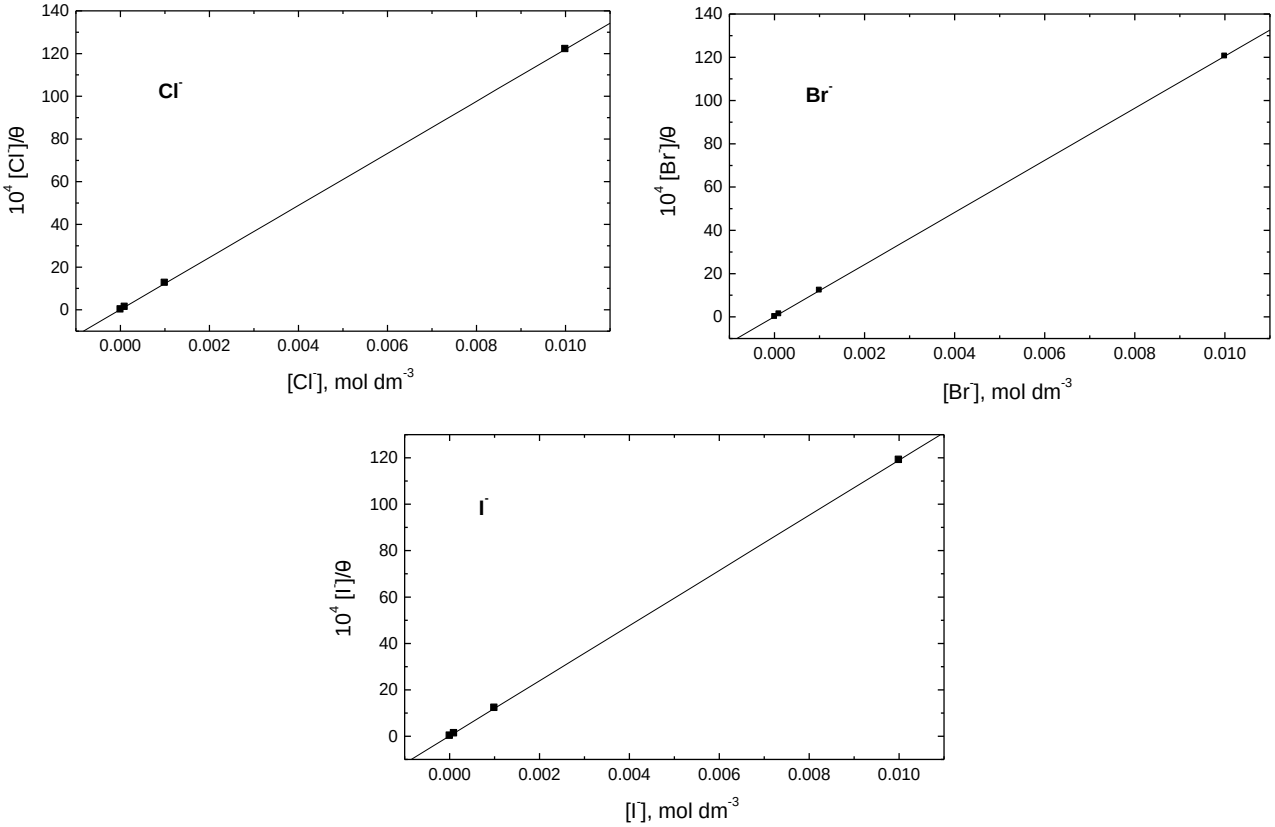

Figure 9 Langmuir adsorption isotherms for SCP and halide ions on mild steel in 0.5 M H_2SO_4 at 25 ºC.

Table 3 Values of K_{ads} and ΔG_{ads} for SCP and halide ions on mild steel in 0.5 M H_2SO_4 at different temperatures.

Temp, K	$10^{-3}K_{ads}$, mol^{-1}	ΔG_{ads}, kJ mol^{-1}
298	73.54	-37.71
308	72.46	-38.94
318	73.53	-40.24
328	76.32	-41.61

The large negative value of ΔG^{o}_{ads} indicates the strong adsorption of the inhibitor. Generally speaking, the energy values of $\Delta G^{o}_{ads} \leq -20$ kJ mol^{-1} are associated with an electrostatic interaction between charged inhibitor molecules and charged metal surface, i.e., physisorption; while those ≥ -40 kJ mol^{-1} involve charge sharing or transfer from the inhibitor molecules to the metal surface to form a coordinate type bond, i.e. chemisorption. Thus in the present case (ΔG^{o}_{ads} *ca.* 40 kJ mol^{-1}) chemisorption is the most probable mode with a small contribution of the physical mode, i.e., charge sharing between the inhibitor and the metal surface forming co-ordinate covalent bond [43].

The activation thermodynamic parameters of steel dissolution namely, the enthalpy of activation (ΔH_{ads}) and entropy of activation (ΔS_{ads}) is obtained from the transition state equation [44]:

$$\ln\left(\frac{I_{corr}}{T}\right) = \left(\frac{-\Delta H_a}{R}\right)\left(\frac{1}{T}\right) + \left[\ln\left(\frac{R}{Nh}\right) + \frac{\Delta S_a}{R}\right] \quad (8)$$

where N and h are Avogadro's number and Plank's constant, respectively. **Figure** 10 shows the relation between $\log(I_{corr} / T)$ vs. 1/T. ΔH_{ads} and ΔS_{ads} were obtained from the slope and intercept, respectively and given in Table 4. The positive sign of ΔH_{ads} reflects the endothermic nature of the dissolution process. The large and negative sign of ΔS_{ads} in the absence and presence of the inhibitor implying that the activated complex in the rate-determining step represents association rather than dissociation, meaning that a decrease in disorder takes place, going from reaction to the activated complex [45].

Table 4 Activation parameters for the corrosion of mild steel in 0.5 M H_2SO_4 in the absence and presence of SCP inhibitor

10^5 [SCP], M	E_a, kJ mol^{-1}	ΔH_{ads}, kJ mol^{-1}	ΔS_{ads}, J mol^{-1} K^{-1}
0	15.16	12.68	-158.29
1	16.17	13.85	-161.21
3	17.41	15.06	-159.13
6	16.85	14.38	-164.30
10	14.30	12.22	-174.23
20	21.32	18.74	-156.0

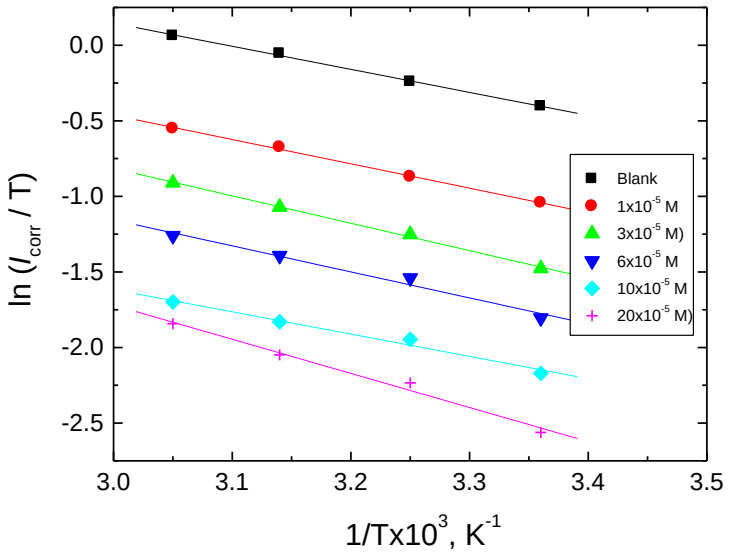

Figure 10 Transition state plots for the corrosion of mild steel in 0.5 M H_2SO_4 in the absence and presence of SCP inhibitor.

Kinetic Parameters for Inhibitor

The dependence of the corrosion rate on temperature is given by the Arrhenius equation:

$$i_{corr} = A\exp\left(\frac{-E_a}{RT}\right) \quad (9)$$

where E_a represents the apparent activation energy, A is the pre-exponential factor, and i_{corr} is the corrosion rate. **Figure** 11 shows the Arrhenius plots of ln i_{corr} vs. $1/T$ in the absence and presence of different concentrations of SCP at different temperature. The values of E_a listed in Table 4 are obtained from the slopes of the Arrhenius plots. The linear regression coefficients of all plots are over 0.99 indicates the validation of the employed kinetic mode. The increase in the values of E_a in the presence of inhibitor indicates a strong adsorption of the inhibitor molecules at the metal surface. It has been reported that [46-48] there are several cases regarding the effect of an inhibitor on the activation energy and inhibition efficiency; 1st case %P decrease with increasing temperature and E_a in the presence of the inhibitor is larger compared with the blank, 2nd case is the reverse to case one, i.e., %P increase with temperature and E_a in the presence of the inhibitor is lower compared with the blank and the third case %P is independent of temperature and E_a values in the absence and presence of inhibitor are the same. In the present case both %P and E_a are slightly affected. Thus follows the third one indicating the efficient inhibition irrespective of the temperature, within the studied temperature rage. The slight increase in the activation energy might classify the adsorption of SCP as a physical one [49-51]. However based on ΔG_{ads} and ΔH_{ads} values the adsorption might be classified as a chemical mode. Therefore, it is concluded that, the adsorption of molecules on the mild steel surface takes place through both physical and chemical processes simultaneously [52].

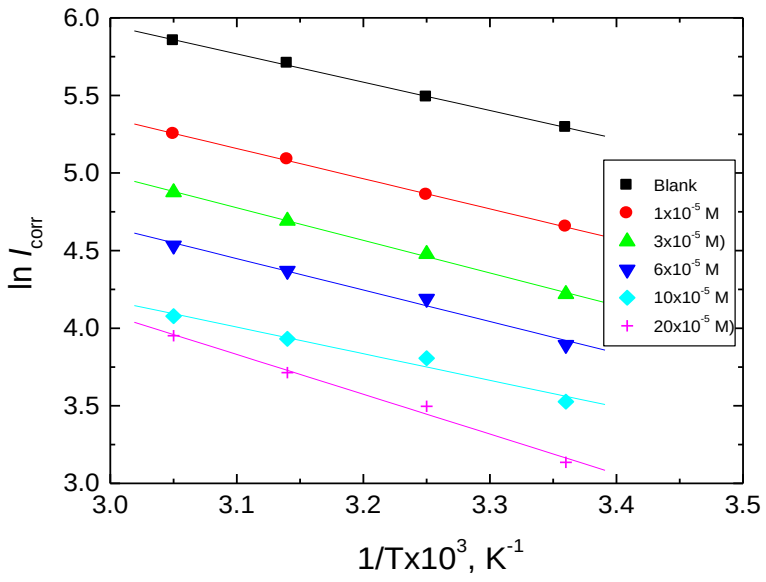

Figure 11 Arrhenius plots for the corrosion of mild steel in 0.5 M H_2SO_4 in the absence and presence of SCP inhibitor.

References

[1] Ali SA, Saeed MT, Rahman SU, Corros Sci 2003, 45, 253-266.
[2] Bentiss F, Lebrini M, Lagrenee M, Corros Sci 2005, 47, 2915–2931.
[3] Lebrini M, Bentiss F, Vezin H, Lagrenée M, Corros Sci 2006, 48, 1279–1291.

[4] Wang L, Corros Sci 2006, 48, 608-616.
[5] Noor E, Corros Sci 2005, 47, 33-55.
[6] Sanyal B, Prog Org Coat 1981, 9, 165-236.
[7] Li X, Deng S, Fu H, Corros Sci 2009, 51, 485-492.
[8] Benabdellah M, Benkaddour M, Hammouti B, Bendahhou M, Aouniti A, Appl Surf Sci 2006, 252, 6212–6217.
[9] Raja PB, Sethuraman MG, Mater Lett 2008, 62, 113–116.
[10] Wang L, Pu J, Luo H, Corros Sci 2003, 45, 677–683.
[11] Cao Z, Tang Z, Cang H, Xu J, Lu G, Jing W, Corros Sci 2014, 83, 292–298.
[12] Radojcic I, Berkovic K, Kovac S, Vorkapic-Furac J, Corros Sci 2008, 50,1498–1504.
[13] Awad MI, J Appl Electrochem 2006, 36, 1163-1168.
[14] Bouklah M, Hammouti B, Benhadda B, Benkadour M, J Appl Electrochem 2005, 35, 1095-1101.
[15] Fouda AS, Al-Sarawy AA, El-Katori EE, Desalination 2006, 201, 1-13.
[16] Fiala A, Chibani A, Darchen A, Boulkamh A, Djebbar K, Appl Surf Sci 2007, 253, 9347-9356.
[17] El-Etre AY, Corros Sci 2001, 43, 1031-1039.
[18] Aksut AA, Bilgic S, Corros Sci 1992, 33, 379–387.
[19] Bilgic S, Aksut AA, Br Corros J 1993, 28, 59–62.
[20] Moretti G, Guidi F, Corros Sci 2002, 44, 1995-2011.
[21] Amin MA, El-Rehim SSA, El-Sherbini EEF, Bayoumy RS, Electrochim Acta 2007, 52, 3588–3600.
[22] Moretti G, Guidi F, Corros Sci 2002, 44, 1995–2011.
[23] Fallavena T, Antonow M, Goncalves RS, Appl Surf Sci 2006, 253, 566–571.
[24] Bouyanzer A, Hammouti B, Majidi L, Mater Lett 2006, 60, 2840–2843.
[25] Rahim AA, Rocca E, Steinmetz J, Kassim MJ, Corros Sci 2008, 50, 1546-1550.
[26] Chauhan LR, Gunasekaran G, Corros Sci 2007, 49, 1143–1161.
[27] Abdel-Gaber AM, Abd-El-Nabey BA, Sidahmed IM, El-Zayady AM, Saadawy M, Corros Sci 2006, 48, 2765–2779.
[28] Khamis A, Saleh MM, Awad MI, Corros Sci 2013, 66, 343-349.
[29] Khamis A, Saleh MM, Awad MI, El-Anadouli BE, Corros Sci 2013, 74, 83-91.
[30] West, JM. Electrodeposition and Corrosion Process, second ed., Van Nostrand-Reinhold, London,1970. p.93.
[31] Lebrini M, Robert F, Roos C, Int J Electrochem Sci 2010, 5, 1698–1712.
[32] Growcock FB, Jasinski RI, J Electrochem Soc 1989,136, 2310–2314.
[33] Shanbhag AV, Venkatesha TV, Praveen PM, Abd-Hamid SB, J Iron Steel Res International, 2014,8, 804-808.
[34] El-Sayed MS, Appl Surf Sci 2014, 292, 190–196.
[35] Qiang Z, Adams C, Water Res 2004, 38, 2874-2890.
[36] Ahmed Y, Musa H, Abdul Amir H, Kadhum AM, Takriff MS, Chee EP, Curr Appl Phys 2012, 12, 325-330.
[37] Jeyaprabha C, Sathiyanarayanan S, Venkatachari G, Electrochim Acta 2006, 51, 4080-4088.
[38] Li X, Deng S, Fu H, Mu G, Corros Sci 2008, 50,3599-4009.
[39] Umeron SA, Ogbobe O, Igweio, Ebenso EE, Corros Sci 2008, 50, 1998-2006.
[40] Yadav DK, Quraishi MA, Ind Eng Chem Res 2012, 51, 8194-8210.
[41] Ebenso EE, Obot IB, Murulana LC, Int J Electrochem Sci 2010, 5, 1574-1586.
[42] Tourabi M, Nohair K, Traisnel M, Jama C, Bentiss F, Corros Sci 2013, 75,123-133.
[43] Moretti G, Guidi F, Grion G, Corros Sci 2004, 46, 387-403.
[44] Bockris JOM, Reddy AKN, Modern Electrochemistry, vol. 2, Plenum Press, New York, 1977.
[45] Marsh J, Advanced Organic Chemistry, 3rd ed., Wiley, Eastern New Delhi, 1988.
[46] Solmaz R, Corros Sci 2014, 79, 169–176.
[47] Li X, Deng S, Fu H, Li T, Electrochim Acta 2009, 54, 4089-4098.
[48] Oguzie EE, Mater Chem Phys 2004, 87, 212-217.
[49] Xu B, Liu Y, Yin X, Yang W, Chen Y, Corros Sci 2013, 74, 206-213.
[50] Anejjar A, Zarrouk A, Salghi R, Zarrok H, Ben Hmamou D, Hammouti B, Elmahi B, Al-Deyab SS, J Mater Environ Sci 2013, 4, 583-592.

[51] Oguzie EE, Adindu CP, Enenebeaku CK, Ogukwe CE, Chidiebere MA, Oguzie KL, J Phys Chem C 2012, 116, 13603-13615.
[52] Tang Y, Zhang F, Huc S, Cao Z, Wu Z, Jing W, Corros Sci 2013, 74, 271-282.

Publication History
Received 01st Jan 2015
Revised 19th Jan 2015
Accepted 16th Feb 2015
Online 28th Feb 2015